CHAPTER

Doubly Fed Induction Generator in Wind Energy Conversion Systems

15

Domingos S.L. Simonetti[1], **Arthur E.A. Amorim**[1], **Flávio D.C. Oliveira**[2]

Electrical Engineering Department, Federal University of Espirito Santo, Vitória, Brazil[1]; *Computation and Electronics Engineering Department, Federal University of Espirito Santo, São Mateus, Brazil*[2]

CHAPTER OUTLINE

Advances in Renewable Energies and Power Technologies. https://doi.org/10.1016/B978-0-12-812959-3.00015-0

1. INTRODUCTION

1.1 HISTORICAL REVIEW OF DOUBLY FED INDUCTION GENERATOR TECHNOLOGY

Wind energy conversion system (WECS) has experienced an expressive development in the past few years. New technologies on turbines, machines, drives, and protection devices have been developed and these devices have been improved progressively. The machine used to convert mechanical rotational energy into electrical energy is the core of any WECS. According to the machine chosen, all other devices are affected; fixed- or variable-speed turbine, power electronic converter type, and the respective power, protections used, and so forth.

Doubly fed induction generator (DFIG) moves together with this technology development. DFIG is nothing more but a wound rotor induction machine, used for years in the past for application requiring speed control. However, working as a generator this machine enables an important feature: it can produce power both in subsynchronous and supersynchronous speeds. Because of this trait, wind turbine is able to operate in a wide range of velocities with high efficiency.

As a characteristic of DFIG, to generate power in subsynchronous speed, the rotor consumes energy. On the other hand, when it is in supersynchronous speed the rotor generates power. Besides that, the frequency of currents produced or consumed in rotor circuit varies according to the rotor speed. To provide the means of such behavior, a bidirectional power electronic converter is used in rotor circuit to be this variable source or load to machine rotor, depending on operation speed. Previously, current source inverter was used, as presented in Smith and Nigim [1]. Nonetheless, this topology produces very poor quality current and has several issues when operating near synchronous speed. To deal with these problems, Pena, Clare, and Asher [2] propose the use of two pulse width modulation (PWM) voltage source converters in a back-to-back structure. The performance with this arrangement is relevant, and it is still used in modern WECS.

1.2 STRUCTURE

The structure of a DFIG-based WECS is formed basically by the wind turbine, the gear box, the wound rotor induction machine, and the back-to-back converter, as

shown in Fig. 15.1. Other peripheral devices are very common, such as the passive filter, the crowbar resistances, and the chopper circuit.

One of the most important advances in WECS technology was the use of variable-speed wind turbines. It is well established that for each wind speed, there is a rotor speed that maximizes power production, as a function of power coefficient [3]. Once wind speed has several variations along the day, this improvement allows a better power extraction, increasing WECS efficiency. The use of variable-speed turbines was only possible because of the advances in power electronics and favored the propagation of DFIG-based WECS.

As wind turbines commonly operate in low speeds and the DFIG turns pretty faster, it is necessary to use a gear box to couple these machine shafts. The transmission is one of the most critical drawbacks of DFIG system, producing losses and requiring frequent maintenance.

As stated before, DFIG is a wound rotor induction machine. This machine is very well-known and there are numerous models to represent its behavior, depending on the analysis conducted. Some of this models used for a better understanding of DFIG will be presented further. Basically, in WECS applications, stator is directly connected to the grid, while rotor is connected to a back-to-back converter.

As a result of the DFIG rotor characteristic of having power being provided or consumed, depending on the situation, the power converter used has to be bidirectional. Besides that, it has to operate with different frequencies in each side, a fixed one (50 or 60 Hz) on the grid side and a variable one on rotor side, determined by the wind speed and the best operation point. It is also desired that this converter produces good quality currents and voltages, with low harmonic content, to prevent machine depreciation and to ensure good energy quality indexes provided to the grid. More details on power electrics converter topologies and features will be presented below.

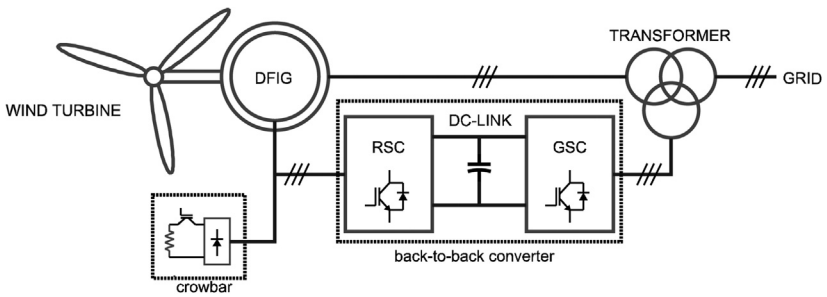

FIGURE 15.1

Doubly fed induction generator (DFIG) basic structure. *GSC*, grid side converter; *RSC*, rotor side converter.

Source: Author.

DFIG stator and rotor voltages usually are not equal because of the machine transformation ratio. Also the produced voltage values do not match the grid voltage. Hence, a three-winding transformer is used to couple these three voltages.

With voltage source converters, to guarantee proper operation, it is necessary to use a passive filter, with dominant inductive behavior. Also, these converters produce voltage harmonics that can disturb other sensitive equipment connected near the wind farm if a proper filter is not adopted to prevent them from flowing [4]. There are countless possibilities for filter design, from filter order, topology, and quality factor to materials used in inductors core.

DFIG is especially susceptible to grid voltage disturbances. To prevent the converter from damages deriving from these transients, some protection devices are commonly applied. To protect converter's switches against high currents on rotor circuit, crowbar resistances are employed. These resistances are normally disconnected from the circuit and when a fault is detected they are inserted in parallel to rotor, providing an alternative path to currents, instead of flow through the converter. A chopper circuit is another protection which prevents high voltages on the converter's DC link. This device consists of a switchable resistance in parallel to DC-link capacitor, which is activated when its voltages surpasses safe values, wasting the extra energy.

1.3 DOUBLY FED INDUCTION GENERATOR SINGULARITIES

Some characteristics of DFIG distinguish it from other WECS. The most important one concerns the converter. Despite using the so-called, full converter—that is, a converter that deals with the full power produced by the turbine—DFIG uses a partial converter—which controls the total power, but just a part of it passes through the converter.

In DFIG system the converter is placed in rotor circuit, while the stator is directly connected to the grid. With this configuration, as will be stated further, only a fraction of the power, proportional to machine slip, will pass through the converter. This is recognized as the main advantage of DFIG system—for the same wind turbine power its converter is reduced, to around 25%, in comparison with other technologies, reducing costs, size, and weight.

Other advantages of DFIG are its wide speed range operation, from 60% up to 110% of rated speed and also the fact that this is an extremely reliable and simple construction machine. On the other hand, this structure leads to some issues for DFIG-based WECS: the machine is directly connected to the grid, which make it extremely susceptible to grid disturbances and faults [5].

Another peculiarity of DFIG is the presence of brushes on rotor circuit. They are necessary to make contact with rotor wounds that, obviously, are turning. This is a drawback, once the brushes need constant maintenance and are a source of failures.

In the following sections, characteristics of DFIG modeling and control will be discussed. Also, the power electronic converters used in WECS equipped with DFIG are presented. In addition, a brief review of new trends on DFIG ride-through to grid disturbances is outlined.

2. MODELING

2.1 DOUBLY FED INDUCTION MACHINE

The doubly fed induction machine (DFIM) is a wound rotor induction machine and has a construction very similar to the traditional squirrel-cage machine. In a concise way, it consists of two three-phase winding sets: stator and rotor, as shown in Fig. 15.2.

The application of symmetric three-phase voltages along with the spatial distribution of the windings in the stator produces a rotating magnetic field in the air gap. Such magnetic field is seen as a time-variant field by each rotor winding, in which AC voltages are induced. The induced rotor voltage and its frequency are proportional to the difference between the stator flux speed and the mechanical rotor speed. In DFIM, rotor windings are also fed by another source, through brushes, which enable some singularities in the machine behavior.

Denoting ω_s as the angular frequency of stator voltages (rad/s) and p as the pairs of poles of the DFIM, the angular frequency of rotor voltages, ω_r, is given by Eq. (15.1):

$$\omega_r = \omega_s - \omega_m \tag{15.1}$$

where ω_m is the angular speed at shaft,

$$\omega_m = \frac{p \cdot V_{\text{RPM}}}{60} \tag{15.2}$$

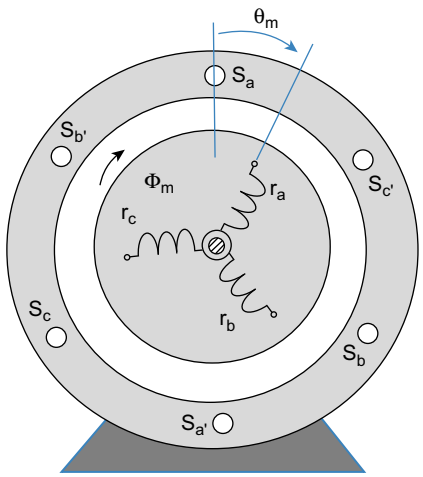

FIGURE 15.2

Simplified doubly fed induction machine. ω_m, mechanical rotational speed at shaft (RPM); s_a, s_b, s_c, r_a, r_b, r_c, stator and rotor windings for phases *a*, *b*, *c* respectively; Φ_m, magnetizing flux.

Source: Author.

The slip is defined as the relation between angular frequencies of rotor and stator voltages:

$$s = \frac{\omega_r}{\omega_s} = \frac{\omega_s - \omega_m}{\omega_s} \rightarrow \omega_r = s \cdot \omega_s \tag{15.3}$$

According to the slip, three different operating modes are possible for the DFIM:

Subsynchronous operation: $\omega_m < \omega_s \Rightarrow s > 0$
Synchronous operation: $\omega_m = \omega_s \Rightarrow s = 0$
Supersynchronous operation: $\omega_m > \omega_s \Rightarrow s < 0$

The stator and rotor voltage equations for a, b, and c windings can be described as in Eq. (15.4) [6]:

$$\begin{aligned} \left[v_{s,abc}\right] &= R_s\left[i_{s,abc}\right] + \frac{d}{dt}\left[\lambda_{s,abc}\right] \\ \left[v_{r,abc}\right] &= R_r\left[i_{r,abc}\right] + \frac{d}{dt}\left[\lambda_{r,abc}\right] \end{aligned} \tag{15.4}$$

and

$$\begin{bmatrix} \lambda_{s,abc} \\ \lambda_{r,abc} \end{bmatrix} = \begin{bmatrix} [L_s] & [L_{sr}] \\ [L_{rs}] & [L_r] \end{bmatrix} \times \begin{bmatrix} i_{s,abc} \\ i_{r,abc} \end{bmatrix} \tag{15.5}$$

where

$$[L_s] = \begin{bmatrix} L_{\sigma s} + L_{ms} & -\frac{1}{2}L_{ms} & -\frac{1}{2}L_{ms} \\ -\frac{1}{2}L_{ms} & L_{\sigma s} + L_{ms} & -\frac{1}{2}L_{ms} \\ -\frac{1}{2}L_{ms} & -\frac{1}{2}L_{ms} & L_{\sigma s} + L_{ms} \end{bmatrix}$$

$$[L_r] = \begin{bmatrix} L_{\sigma r} + L_{mr} & -\frac{1}{2}L_{mr} & -\frac{1}{2}L_{mr} \\ -\frac{1}{2}L_{mr} & L_{\sigma r} + L_{mr} & -\frac{1}{2}L_{mr} \\ -\frac{1}{2}L_{mr} & -\frac{1}{2}L_{mr} & L_{\sigma r} + L_{mr} \end{bmatrix} \tag{15.6}$$

$$[L_{sr}] = [L_{rs}]^T = L_m \begin{bmatrix} \cos\theta_m & \cos\left(\theta_m + \frac{2\pi}{3}\right) & \cos\left(\theta_m - \frac{2\pi}{3}\right) \\ \cos\left(\theta_m - \frac{2\pi}{3}\right) & \cos\theta_m & \cos\left(\theta_m + \frac{2\pi}{3}\right) \\ \cos\left(\theta_m + \frac{2\pi}{3}\right) & \cos\left(\theta_m - \frac{2\pi}{3}\right) & \cos\theta_m \end{bmatrix}$$

where $v_{s,abc}$ and $v_{r,abc}$, stator and rotor voltages for phases a, b, and c respectively; $i_{s,abc}$ and $i_{r,abc}$, stator and rotor c for phases a, b, c; R_s and R_r, stator and rotor resistances; $L_{\sigma s}$, $L_{\sigma r}$, stator leakage and rotor leakage inductance; L_{ms}, L_{mr}, stator to stator and rotor to rotor mutual inductance; L_m, maximum value of the stator−rotor mutual inductance.

The drawback of this complete *abc* representation is that a large set of equations are derived needing much effort to accomplish the analysis.

2.2 THE STATIC MODEL

The steady-state−equivalent electric circuit of the machine is developed through physics equations that describe the machine behavior. This modeling allows an evaluation of machine performance and its operating modes.

2.2.1 Equivalent Circuit

A representative steady-state −equivalent electric circuit of the DFIM is obtained considering the following assumptions:

- The stator and the rotor are connected in the star configuration;
- The stator is powered by the grid with constant and balanced three-phase AC voltage amplitude and constant frequency;
- The rotor is powered by the grid with constant and balanced three-phase AC voltage amplitude and constant frequency;

Fig. 15.3 represents one phase of the stator and rotor three-phase windings.

2.2.2 Referring Rotor to Stator

The magnetic field of the stator rotates at a speed synchronized to the grid frequency. The magnetic field of the rotor rotates synchronized to rotor currents frequency. Despite this, at the machine air gap the rotor field is superimposed to the mechanical

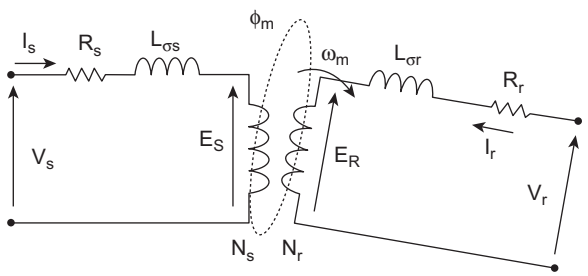

FIGURE 15.3

Steady-state−equivalent electric circuit. I_s, stator current; E_S, induced electro-magnetic force in the stator; I_r, rotor current; L_M, magnetizing inductance, $L_M = 3L_{ms}/2$; N_s, N_r, stator and rotor winding's number of turns.

Source: Author.

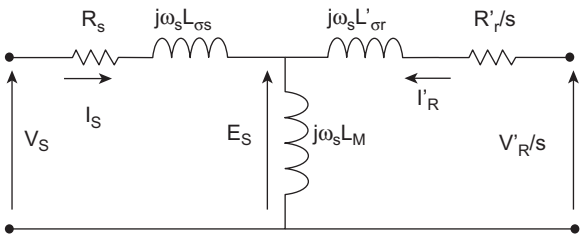

FIGURE 15.4

Steady-state—equivalent circuit of the doubly fed induction machine referred to the stator with stator frequency. $a = \frac{N_s}{N_r}$; $R'_r = a^2 R_r$; $L'_{\sigma r} = a^2 L_{\sigma r}$; $V'_r = aV_r$; $I'_r = \frac{I_r}{a}$.

Source: Author.

speed. Therefore, stator windings see the rotor field at its own synchronous frequency. In this way, to perform the analysis, it is advantageous to represent all circuits referred to stator as presented in Fig. 15.4 [7].

2.2.3 Doubly Fed Induction Machine Operation Modes

DFIM can operate as a generator as well as a motor in both subsynchronous or supersynchronous speeds.

The relation between stator and rotor power can be deduced, considering that the sum of the active power (P) in a closed system is equal to zero ($\sum P = 0$). Considering P_m as the shaft mechanical power, P_S the stator active power, P_R the rotor active power, and P_{loss} the active power losses (copper losses, neglecting core losses), we have:

$$P_m = P_S + P_R + P_{loss} \tag{15.7}$$

It is well known that [7]:

$$P_R = -s \cdot P_S \tag{15.8}$$

So, neglecting power losses ($P_{loss} \approx 0$):

$$P_m = (1 - s) \cdot P_S \tag{15.9}$$

2.2.3.1 Motor Operation ($P_m > 0$)

The machine is delivering mechanical power and receiving electric power from grid, as shown in Fig. 15.5.

Speed	P_m	P_S	P_R
Subsynchronous: $s > 0$ and $\omega_m < \omega_s$	$P_m > 0$	$P_S > 0$	$P_R > 0$
Supersynchronous: $s < 0$ and $\omega_m > \omega_s$	$P_m > 0$	$P_S > 0$	$P_R < 0$

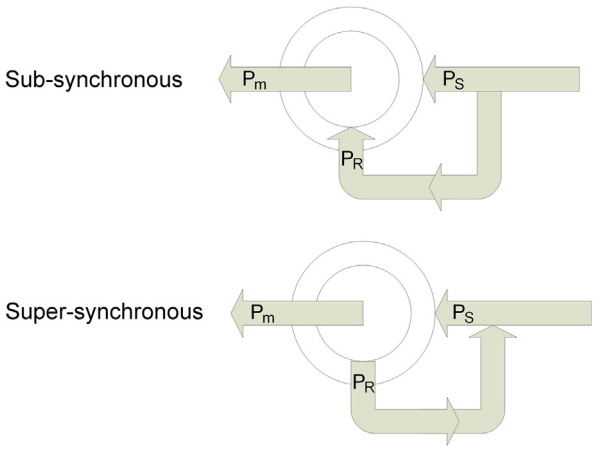

FIGURE 15.5

Active power flow representation for motor operation.

Source: Author.

2.2.3.2 Generator Operation ($P_m < 0$)

The machine is receiving mechanic power and delivering electric power from grid, as shown in Fig. 15.6:

Speed	P_m	P_S	P_R
Subsynchronous: $s > 0$ and $\omega_m < \omega_s$	$P_m < 0$	$P_S < 0$	$P_R > 0$
Supersynchronous: $s < 0$ and $\omega_m > \omega_s$	$P_m < 0$	$P_S < 0$	$P_R < 0$

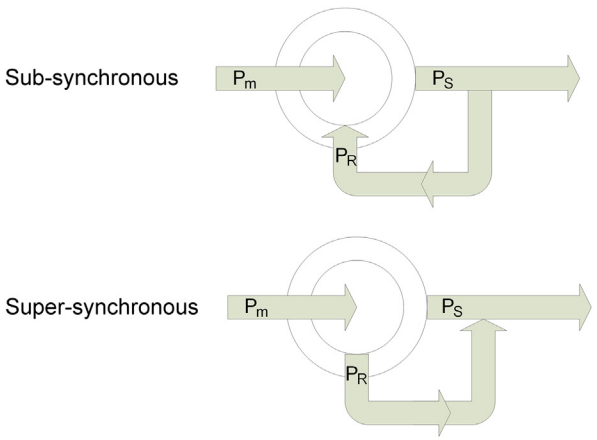

FIGURE 15.6

Active power flow representation for operation as generator.

Source: Author.

2.3 THE DYNAMIC MODELING

Although the steady-state model is useful to understand and for calculus under steady-state, transient operation requires a more complete model to represent the asymmetric coupling effects. In the *abc* frame, a large set of equations are derived needing much effort to accomplish the analysis.

2.3.1 Reference Frame Transformation

Consider the equations of a symmetric three-phase system:

$$\begin{aligned} x_A(t) &= X\cdot\cos(\omega\cdot t+\phi) \\ x_B(t) &= X\cdot\cos\left(\omega\cdot t+\phi\ -\frac{2\pi}{3}\right) \\ x_C(t) &= X\cdot\cos\left(\omega\cdot t+\phi+\frac{2\pi}{3}\right) \end{aligned} \tag{15.10}$$

As the symmetric three-phase system is linearly dependent $(x_a(t) = -x_b(t) - x_c(t))$, it can be represented by an equivalent two-phase orthogonal system, as shown in Fig. 15.7. The new reference frame is also called $\alpha\beta$ transformation, $x_a(t)$, $x_b(t)$, and $x_c(t)$ are transformed to $x_\alpha(t)$ and $x_\beta(t)$.

This representation transforms the models and their equations in simpler elements than the classic three-phase model. In the $\alpha\beta$ frame, $x_\alpha(t)$ and $x_\beta(t)$ can be composed in a time-dependent phasor $x_{\alpha\beta}(t)\angle\theta$. The mathematical transformation is given by Eq. (15.11):

$$\begin{bmatrix} x_\alpha \\ x_\beta \end{bmatrix} = \frac{2}{3}\cdot\begin{bmatrix} 1 & \frac{-1}{2} & \frac{-1}{2} \\ 0 & \frac{\sqrt{3}}{2} & \frac{-\sqrt{3}}{2} \end{bmatrix}\cdot\begin{bmatrix} x_a \\ x_b \\ x_c \end{bmatrix} \tag{15.11}$$

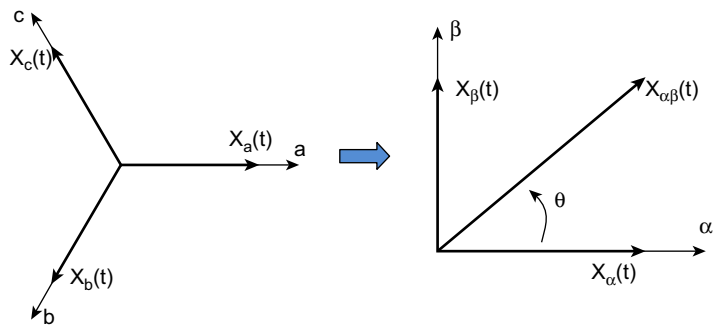

FIGURE 15.7

$\alpha\beta$ Frame.

Source: Author.

Then, one step ahead is to compose the $\alpha\beta$ system at a generic two-phase frame, the so-called dq frame (Park transformation). The generic dq frame can be fixed and coincident to the $\alpha\beta$ frame, or can rotate at any angular speed, but usually it is grid synchronized ($\phi = \omega t$). Fig. 15.8 shows $\alpha\beta$ and dq frame, and Eqs. (15.12) and (15.13) present $\alpha\beta \rightarrow dq$ transformation tied to the grid voltages, considering $v_a = \sqrt{2} \cdot V_{\text{RMS}} \cdot \cos(\omega t)$.

$$\begin{bmatrix} x_d \\ x_q \end{bmatrix} = \begin{bmatrix} \cos\phi & \text{sen}\phi \\ -\text{sen}\phi & \cos\phi \end{bmatrix} \cdot \begin{bmatrix} x_\alpha \\ x_\beta \end{bmatrix} \tag{15.12}$$

$$\varnothing = \omega_s t$$

$$v_{s,\alpha} = v_a$$

$$\begin{bmatrix} v_{s,d} \\ v_{s,q} \end{bmatrix} = \begin{bmatrix} \sqrt{2V_{\text{rms}}} \\ 0 \end{bmatrix} \tag{15.13}$$

2.3.2 Dynamic Modeling

The grid-synchronized dq transformation can be applied to the set of equations given by Eqs. (15.4)–(15.6), generating a simpler but effective complete dynamic circuit model, which is shown in Fig. 15.9.

Neglecting the power losses associated with the stator and rotor resistances, the powers and electromagnetic torque (T_{em}) equation are given by Eqs. (15.14)–(15.18).

$$P_s = \frac{3}{2}\left(v_{s,d} i_{s,d} + v_{s,q} i_{s,q}\right) \tag{15.14}$$

$$P_r = \frac{3}{2}\left(v_{r,d} i_{r,d} + v_{r,q} i_{r,q}\right) \tag{15.15}$$

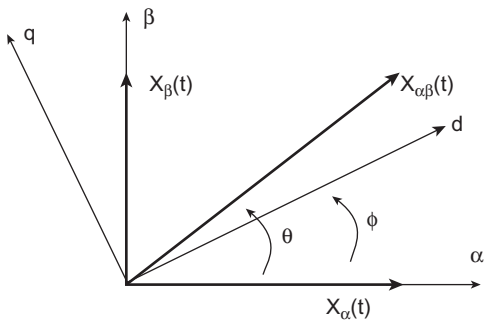

FIGURE 15.8

$\alpha\beta \rightarrow dq$ Transformation.

Source: Author.

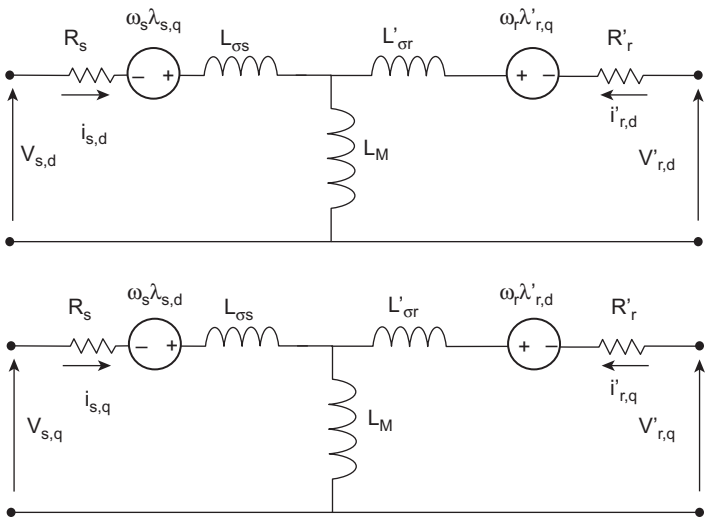

FIGURE 15.9

The *dq* equivalent circuit. $\lambda_{s,d} = (L_{\sigma s} + L_M)i_{s,d} + L_M i'_{r,d}$; $\lambda_{s,q} = (L_{\sigma s} + L_M)i_{s,q} + L_M i'_{r,q}$; $\lambda'_{r,d} = (L'_{\sigma r} + L_M)i'_{r,d} + L_M i_{s,d}$; $\lambda'_{r,q} = (L'_{\sigma r} + L_M)i'_{r,q} + L_M i_{s,q}$.

Source: Author.

$$Q_s = \frac{3}{2}\left(v_{s,q}i_{s,d} - v_{s,d}i_{s,q}\right) \tag{15.16}$$

$$Q_r = \frac{3}{2}\left(v_{r,q}i_{r,d} - v_{r,d}i_{r,q}\right) \tag{15.17}$$

$$T_e = \frac{3}{2}\frac{p}{2}L_M\left(i_{s,q}i'_{r,d} - i_{s,d}i'_{r,q}\right) \tag{15.18}$$

2.4 MODEL FOR GRID DISTURBANCES

2.4.1 The Complex Vector Representation

Considering v_a, v_b, and v_c, a symmetric set of three-phase voltages, namely $v_a(t) = \sqrt{2}V_{\text{rms}}\cos(\omega t)$, $v_\alpha(t)$, and $v_\beta(t)$ from Eq. (15.11), can be composed as a time-dependent phasor, $v_{\alpha\beta}(t) \angle \theta$ in a polar form. Considering the Euler formula, the phasor can be expressed as a complex vector:

$$v_{s,\alpha\beta}(t)\angle\varnothing = \overrightarrow{v_s} = \sqrt{2}V_{\text{rms}}e^{j\omega_s t} \tag{15.19}$$

2.4.2 Doubly Fed Induction Generator Behavior Under Symmetrical Voltage Dips

Among all fault situations, the symmetrical one is that which leads to higher fault currents. This is because the analysis carried out here only considers this situation.

When a voltage dip happens, there is an imbalance between the former magnetic flux operating on machine and the new imposed stator voltage. With this abrupt change on grid voltage, two flux components, named forced and natural, arise in the magnetic flux. The forced component is proportional to the new grid voltage, while the natural component represents the transitory phase between these two states, describing machine demagnetization process. The transient operation of the stator flux induces high voltages on the rotor circuit, which is very dangerous for the power electronics converter connected to the rotor.

The stator flux linkage Ψ_s, using complex vector representation, can be obtained from:

$$\frac{d\vec{\psi}_s(t)}{dt} = \vec{v}_s(t) - R_S \cdot \vec{i}_s(t) \tag{15.20}$$

The generator is initially considered at normal operation, and at $t = 0$ s, a voltage dip occurs with depth D, as shown in Fig. 15.10. Eq. (15.21) describes the grid voltage before and after the voltage dip.

$$\vec{v}_s(t) = \begin{cases} V_p \cdot e^{j \cdot \omega_s \cdot t} & t < 0\ s \\ (1 - D) \cdot V_p \cdot e^{j \cdot \omega_s \cdot t} & t \geq 0\ s \end{cases} \tag{15.21}$$

The ordinary differential equation solution is divided into two terms, the homogeneous solution, Eq. (15.22) and the particular solution, Eq. (15.23):

$$\vec{\psi}_{s\,h}(t) = \frac{D \cdot V_p}{j \cdot \omega_s} e^{-t/\tau_s}, \quad \forall t \geq 0 \tag{15.22}$$

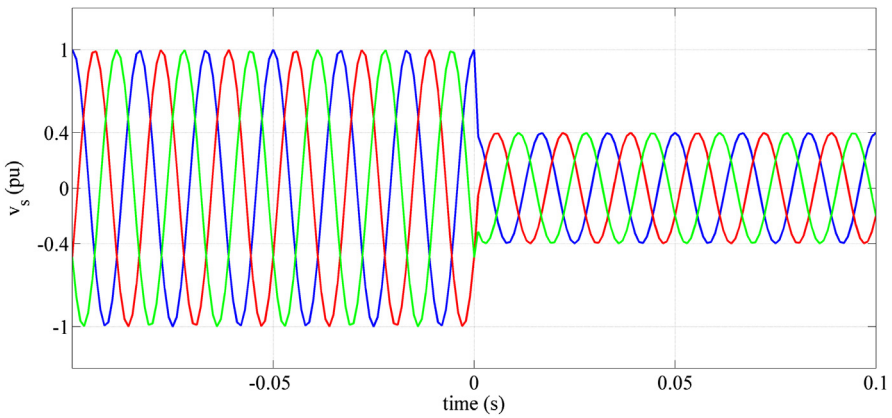

FIGURE 15.10

Voltage dip.

Source: Author.

$$\vec{\psi}_{s\,p}(t) = \frac{(1-D)\cdot V_p}{j\cdot\omega_s} e^{j\cdot\omega_s\cdot t}, \quad \forall\ t \geq 0 \tag{15.23}$$

The homogeneous solution of the magnetic flux is a transient flux and the particular solution is the steady-state component. When the voltage dip occurs, the stator flux has its dynamic as shown in Fig. 15.11 and is described by Eq. (15.24).

$$\vec{\psi}_s(t) = \begin{cases} \dfrac{V_p}{j\cdot\omega_s} e^{j\cdot\omega_s\cdot t} & t < 0 \\ \dfrac{(1-D)\cdot V_p}{j\cdot\omega_s} e^{j\cdot\omega_s\cdot t} + \dfrac{D\cdot V_p}{j\cdot\omega_s} e^{-t/\tau_s} & t \geq 0 \end{cases} \tag{15.24}$$

where

$$\tau_s = \frac{L_S}{R_S}$$

The induced electromagnetic force in the rotor circuit is obtained from Eq. (15.25):

$$\vec{e}_r(t) = \frac{1}{a}\frac{L_m}{L_S}\frac{d\vec{\psi}_r(t)}{dt} \tag{15.25}$$

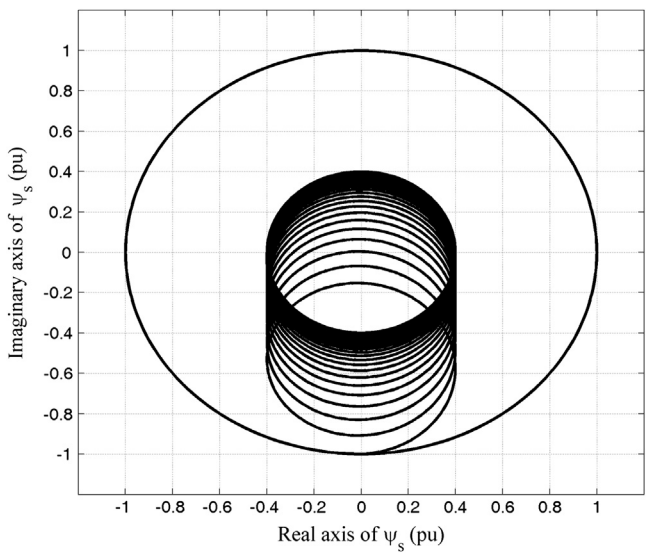

FIGURE 15.11

Stator flux trajectory with *D* voltage dip.

Source: Author.

But the rotor flux Ψ_r is given by:

$$\overrightarrow{\psi}_r(t) = \overrightarrow{\psi}'_s(t) = \overrightarrow{\psi}_s(t)\cdot e^{-j\cdot\omega_m\cdot t}$$

$$= \begin{cases} \dfrac{V_p}{j\cdot\omega_s} e^{j\cdot\omega_r\cdot t} & t < 0 \\ \dfrac{(1-D)\cdot V_p}{j\cdot\omega_s} e^{j\cdot\omega_r\cdot t} + \dfrac{D\cdot V_p}{j\cdot\omega_s} e^{-j\cdot\omega_m\cdot t}\cdot e^{-t/\tau_s} & t \geq 0 \end{cases} \tag{15.26}$$

Using both equations, the induced electromagnetic force in the rotor is obtained as follows:

$$\overrightarrow{e}_r(t) = \begin{cases} \dfrac{1}{u}\dfrac{L_m}{L_S} V_p\cdot s\cdot e^{j\cdot\omega_r\cdot t} & t < 0 \\ \dfrac{1}{u}\dfrac{L_m}{L_S} V_p\cdot\left[(1-D)\cdot s\cdot e^{j\cdot\omega_r\cdot t} - D\cdot(1-s)\cdot e^{-j\cdot\omega_m\cdot t}\cdot e^{-t/\tau_s}\right] & t \geq 0 \end{cases} \tag{15.27}$$

From this last deduction, it can be seen that the induced internal rotor voltage because of a stator voltage dip presents two superposed frequencies, one is function of the slip frequency and the other is associated to the rotational mechanical speed.

The Fig. 15.12 shows the simulation result of the internal voltage e_r of a 2 MW DFIG under a 50% voltage dip. The induced rotor voltage is more than twice its steady-state value. It is possible to see the two superposed frequencies commented

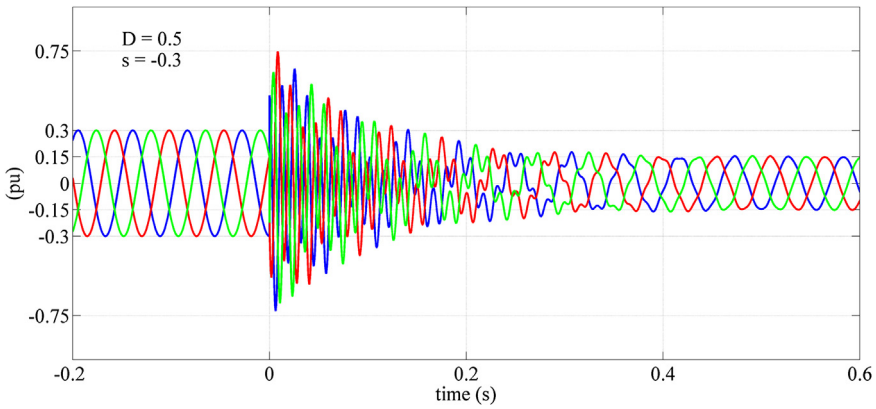

FIGURE 15.12

Rotor-induced voltage during a voltage dip.

Source: Author.

above. This overvoltage produces high-value currents in the rotor circuit, which can seriously damage the rotor converter if some action is not taken.

3. CONTROL SYSTEM

Control system has the task to extract maximum power from the wind. This dynamic control of the DFIG is executed by the adequate control of the power converter. The converter enables variable-speed operation of the wind turbine, decoupling rotor mechanical speed from the power system electrical system. Typically, the behavior of a wind turbine power extraction from wind speed is described by the curves in Fig. 15.13.

For each wind speed, there is a curve of the generator power in function of the generator speed. The maximum power curve can be extracted connecting the maximum Cp points of each curve; the control system aim is to keep the turbine on this curve as the wind varies. However, converter has a limited capacity; thus, it is not possible to obtain optimum power extraction over all wind speeds. It is common to have on wind turbines the curve divided in sections. For very low wind speeds (A-B) the system operates at a constant rotational speed. In section (B-C), the system follows the optimal curve, until machine limitation, when Cp diverges from its optimal point (C-D). For very high wind speeds (D-E), aerodynamic control limits the power extraction to ensure safe conditions for torque in the shafts.

DFIG control is completely done through its rotor, where the power electronic converter is connected. The converter is a back-to-back type, formed by two voltage source converters linked by a DC capacitor. The rotor side converter (RSC) controls

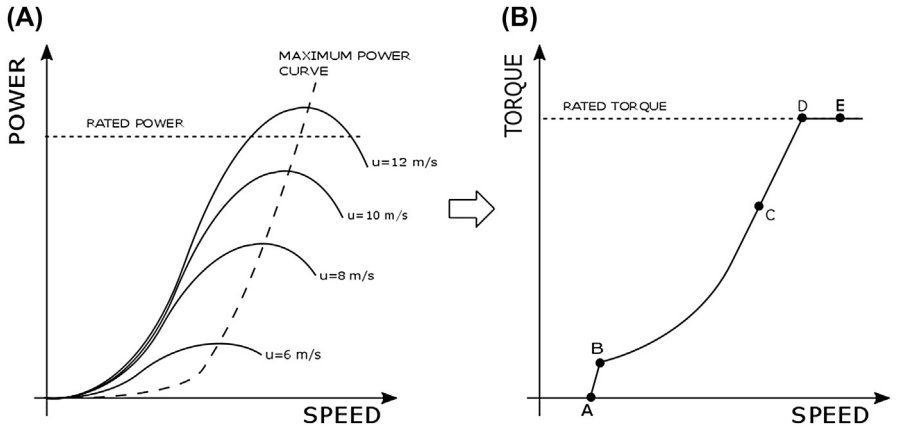

FIGURE 15.13

Wind turbine characteristic for maximum power extraction.

Source: Author.

the DFIG's rotor currents. By these currents, it is possible to control the power flow on machine's stator. In turn, the grid side converter (GSC) controls DC-link voltage and reactive power flow between converter and electrical power system. DC-link capacitor insulates both sides of the back-to-back and damps power fluctuation, acting as an inertia for the rotor power flow.

The control system is primordial for the proper operation of any machine drive; in WECS it is not different. The control of DFIG has to ensure system stability and optimal operation. To do so, there are several variables to be kept controlled in established set points, such as torque, active and reactive powers, and also magnitudes related to the GSC, such as the reactive power and the DC bus voltage. Control system has the task to receive all these references and determine the voltages to be generated in both sides of the back-to-back converter.

3.1 VECTOR CONTROL

The most common strategy for a grid-connected DFIG is the vector control, which is very similar to the widespread classical vector control employed in induction machine drives. As explained in the previous section, if the machine is represented in a synchronous reference frame (dq), active and reactive stator power can be controlled independently, by means of direct and quadrature current. To ensure this decoupled control, it is very important to correctly align the dq reference frame. In the literature, two orientations are discussed, each one has advantages and disadvantages; the first is called flux orientation and the second voltage orientation.

Following the legacy of machine drive's vector control, flux orientation was the first option in DFIG control. With this approach, the machine stator flux is estimated and aligned to the d axis of the reference frame. Another option, discussed later, is the grid voltage orientation. A phase-locked loop is used to detect the angle of the fundamental voltage, which is aligned to the reference frame axis. Both options are equivalent if the stator voltage and flux are stable. In general, stator resistance is very small and the voltage drop on it is negligible, which made both reference frames coincident. Applications using these approaches are found in literature.

The differences are noted during transition, when the phase shift between the stator voltage and the flux are not precisely 90 degrees anymore. Also, Petersson [8] compares both orientation techniques performance and proves that voltage orientation is always stable, although flux orientation may destabilize vector control depending on the d-axis component of the current.

3.2 CONTROL OF GRID SIDE CONVERTER

As shown in Fig. 15.1, one part of the back-to-back converter is called the GSC. GSC is in charge to control DC-link voltage and reactive power flux between the converter and the electrical grid. This is done by means of a cascade control loop,

as shown in Fig. 15.14. In an external loop, these variables are set as references, compared with its measured values and the control gives the reference currents to the internal loop. In the internal loop, reference currents are compared to the measured ones to set the voltages to be produced by converter. To decouple d and q components of control system, a feed-forward loop inserts these compensations on reference voltage.

Usually, proportional integral (PI) controllers are used in both internal and external loops. Basically, the outer loop has two distinct characteristics, one for DC-link voltage control and other to reactive power exchange. DC-link voltage control is done by the balance of active power flowing through GSC and RSC. The relation between the DC-voltage and the current is established by the DC-link capacitance. Reactive power is calculated by measured currents and voltages and is filtered before being inserted in the control loop. For the inner loop, the plant is modeled by the difference between the grid voltage and the converter voltage in filter impedance, which enables PI controller design for better results in currents dynamics.

3.3 CONTROL OF ROTOR SIDE CONVERTER

Active and reactive power flow between the stator and grid are controlled by the RSC. As in GSC, these variables are controlled by means of cascade control loops, as shown in Fig. 15.15. In the same way, external loop set references, compare with measured values and the control gives the reference currents to the internal loop. Internal loop compares reference currents with measured values to set the voltages to

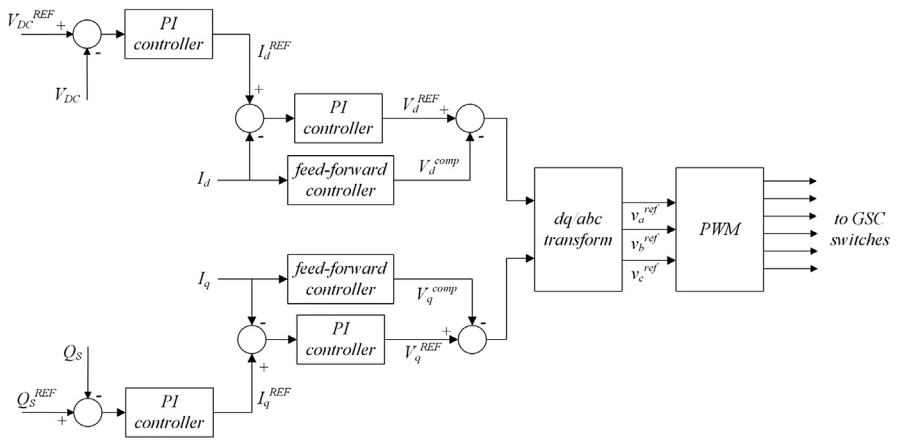

FIGURE 15.14

Control loop for grid side converter.

Source: Author.

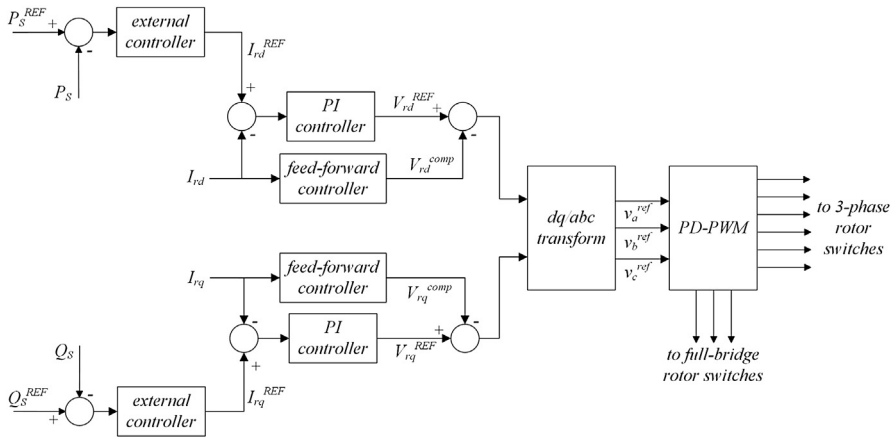

FIGURE 15.15

Control loop for rotor side converter.

Source: Author.

be produced by converter. Feed-forward controllers insert compensations to decouple d and q components in the voltages.

Eqs. (15.4) and (15.5) show the relation between stator and rotor variables. Active and reactive powers in stator are determined by voltages and currents on stator, and the voltages are fixed by electrical grid. Power is controlled by controlling the currents. The stator currents, in turn, can be controlled by rotor currents, which are produced by the RSC. Thus, rotor current control is the ultimate goal of RSC control loops.

According to the *dq* model of DFIG, the reference rotor currents can be evaluated to generate the desired stator power, as shown in Fig. 15.16.

Also, according to the model, oriented by stator voltage, the equations of rotor voltages can be written as:

$$v_{r,d} = R_r i_{r,d} - \omega_r \sigma L_r i_{r,q} + \sigma L_r \frac{d}{dt} i_{r,d} + \frac{L_m}{L_s} \frac{d}{dt} \lambda_{s,d} \tag{15.28}$$

$$v_{r,q} = R_r i_{r,q} - \omega_r \sigma L_r i_{r,d} + \sigma L_r \frac{d}{dt} i_{r,q} + \omega_r \frac{L_m}{L_s} \lambda_{s,d} \tag{15.29}$$

where

$$\sigma = 1 - \frac{L_m^2}{L_s \cdot L_r}$$

These equations are used to model the plant for the inner loop controller design. The last term depends only on stator voltage; thus, it is seen as a perturbation from the control point of view. The cross terms are compensated by feed-forward controllers.

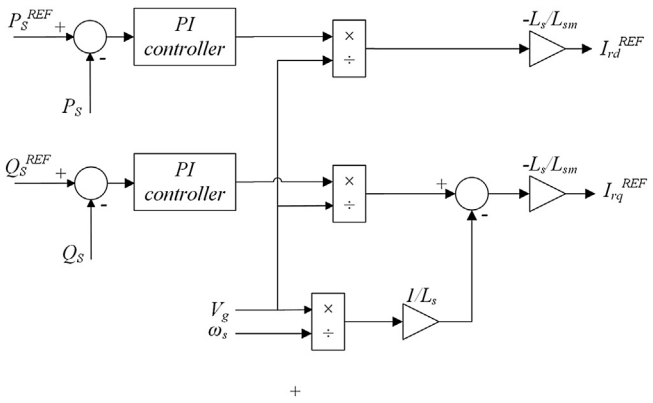

FIGURE 15.16

External control loop for power control.

Source: Author.

4. POWER ELECTRONIC CONVERTERS

The key to correctly operate the induction machine as a double-fed generator is the electronic converter required to connect the rotor terminals to the grid. The converter has the function of adjusting rotor frequency to the frequency of the grid and, at the same time, provides control of active and reactive power that is sent to the line. The converter is about 30% of rated DFIG power. Besides the interconnection structure, other topologies are present in the rotor circuit to protect the main converter.

The most common solution to connect both DFIG rotor and stator (grid) is the well known back-to-back voltage source converter, allowing a four-quadrant operation.

4.1 THE BACK-TO-BACK VOLTAGE SOURCE CONVERTER

The back-to-back structure is composed of two voltage-source converters linked by the same DC-bus [9]. Fig. 15.17 shows the structure using a two-level PWM converter.

The converter is able to synthesize voltages matching rotor requirements on the rotor side and grid requirements on the other side. Despite the fact that usually the stator—rotor turns ratio boosts the rotor voltage with respect to the stator voltage, the slip range of operation is between −0,3 and +0,3, and a not high voltage value is needed to be synthesized on the rotor side. On the grid side, a transformer connection matches voltage values to grid.

Drive signals are generated using sinusoidal PWM (SPWM) (voltage references compared with triangular carrier at switching frequencies), or using space vector modulation (SVPWM). The first is of simpler achievement, but the converter

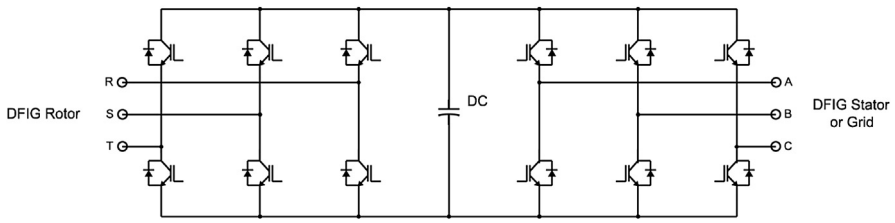

FIGURE 15.17

Two three-phase inverters back to back connected. *DFIG*, doubly fed induction generator.

Source: Author.

potential is subutilized. Some improvement can be done using third-harmonic injection technique. On the other hand, SVPWM allows a better voltage synthesis and better converter utilization but it is more toilsome to implement.

In the last few years, preference has been given to employ neutral-point clamped converters (NPC), in medium-to-high power converters [10]. The NPC, shown in Fig. 15.18, is a multilevel converter that presents lower harmonics in the synthesized voltage, less voltage stress for the same converter compared to the conventional on, and high efficiency.

4.2 THE CROWBAR AND THE CHOPPER

The crowbar is a cost-effective structure to protect the back-to-back converter against high circulating currents during severe voltage dips. As has been shown previously, during a voltage dip, a transient voltage of high value is induced from stator to rotor circuit. This induced voltage leads to high currents on the rotor circuit.

To protect the structure, an alternative current path is created between the DFIG rotor and the RSC, as shown in Fig. 15.1. The main topologies to implement such path are shown in Fig. 15.19. As soon as a voltage dip is detected, drive signals

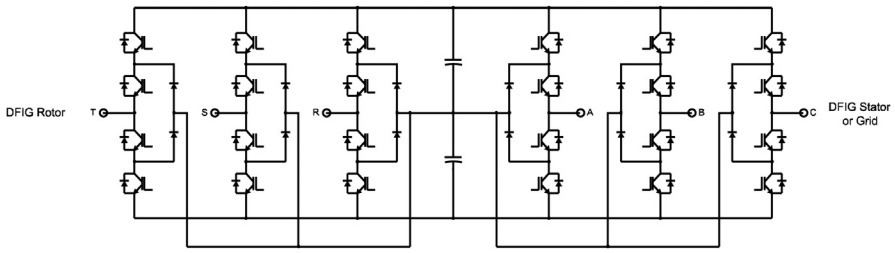

FIGURE 15.18

Neutral-point clamped converters in a back-to-back connection. *DFIG*, doubly fed induction generator.

Source: Author.

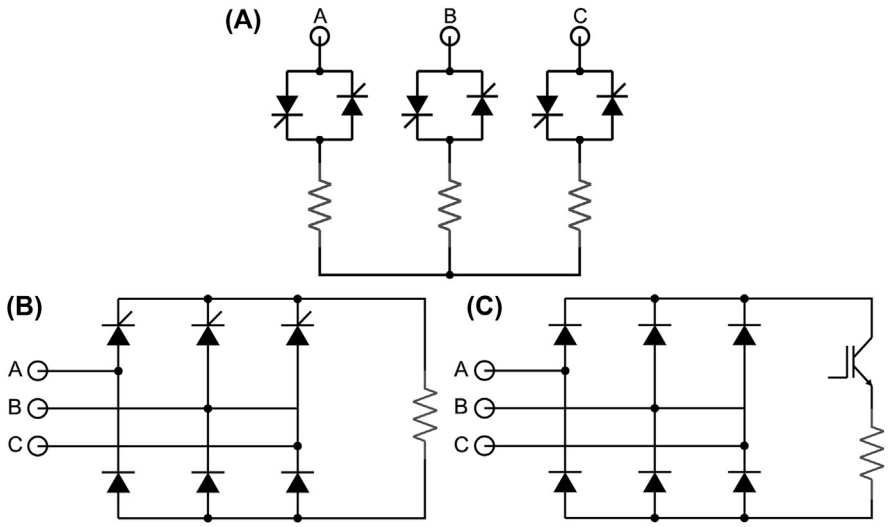

FIGURE 15.19

Topologies for crowbar implementation. (A) with SCR, (B) with SCR + Diodes, (C) with Diodes + IGBT.

Source: Author.

to RSC are turned off, and the crowbar is turned on. At the time the transient finishes, the crowbar is disconnected and the drive signals can be sent again to RSC [11]. The deactivation of the RSC is a drawback of this solution, because the DFIG loses its controllability [12].

Because of the fact that thyristors and diodes support well over current values, topologies (A) and (B) are more robust but are not fully controllable. The topology employing the insulated gate bipolar transistor (IGBT) is fully controllable (it turns on and off exactly with the drive signal), but is more sensitive to overcurrent and overvoltages.

The chopper, shown in Fig. 15.20, is required to protect the converter from overvoltages in the DC link. Such overvoltage can occur mainly during voltage dips. As the drive signals to RSC are cancelled, the converter acts as a diode bridge rectifier. If the voltage at crowbar terminals is greater than DC-voltage, the diode-bridge conducts, delivering power to the capacitor of the DC-link. If the capacitor voltage surpasses a safe limit, the chopper is triggered to discharge the capacitor.

4.3 NEW TRENDS/NOVEL STRUCTURES

The rated power of wind DFIG machines is increasing more and more. To deal with this new reality, novel solutions are being proposed. Matrix converters are being considered [13]; their main advantage is the absence of DC capacitors. Modular

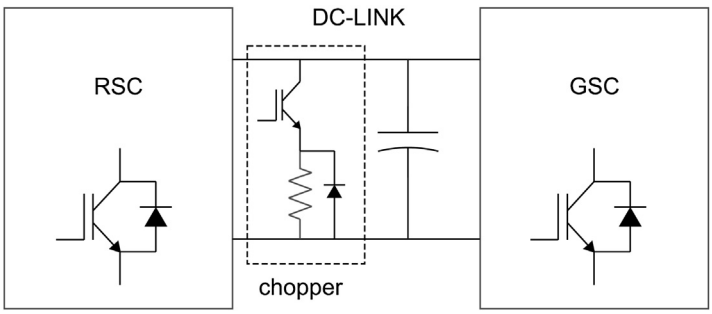

FIGURE 15.20

Chopper circuit. *GSC*, grid side converter; *RSC*, rotor side converter.

Source: Author.

multilevel converters are easy to implement and, using present devices, can process higher power [14]. Parallel connection of converters also can deliver more power in a modular way [13].

5. LOW-VOLTAGE RIDE-THROUGH

5.1 EFFECTS OF VOLTAGE DIP ON DOUBLY FED INDUCTION GENERATOR

As stated in the sections above, the voltage dip is a great issue for the DFIG to deal with. The converter is the most susceptible part of a DFIG-based WECS; hence, the major worries concern voltage dips supportability. The effects of a voltage dip without any countermeasure are tremendous. As in the study by Erlich, Wrede, and Feltes [15], an analysis of this phenomenon is evaluated in this condition. Fig. 15.21 presents the impact of an 80% voltage dip in the most important variables of DFIG—stator voltage; stator, rotor, and GSC currents; DC-link voltage; and stator power.

With the abrupt change in stator voltage, Fig. 15.21 shows that DC components increase the stator currents, as explained before. On the rotor side, these DC components appear as a high-frequency component surpassing the steady-state currents on this circuit. It could be noticed that the levels reached by the rotor currents are extremely higher than the nominal ones. This is unfeasible to deal because of converter switches limitations.

When these high currents flow into the converter, they cause the DC-link voltage to increase. Even if the capacitor is acting in inertia, it is not capable to considerably reduce this behavior on the voltage. Without other countermeasures, DC-link voltage can reach two times its rated value, which is far beyond capacitor and switch design limits.

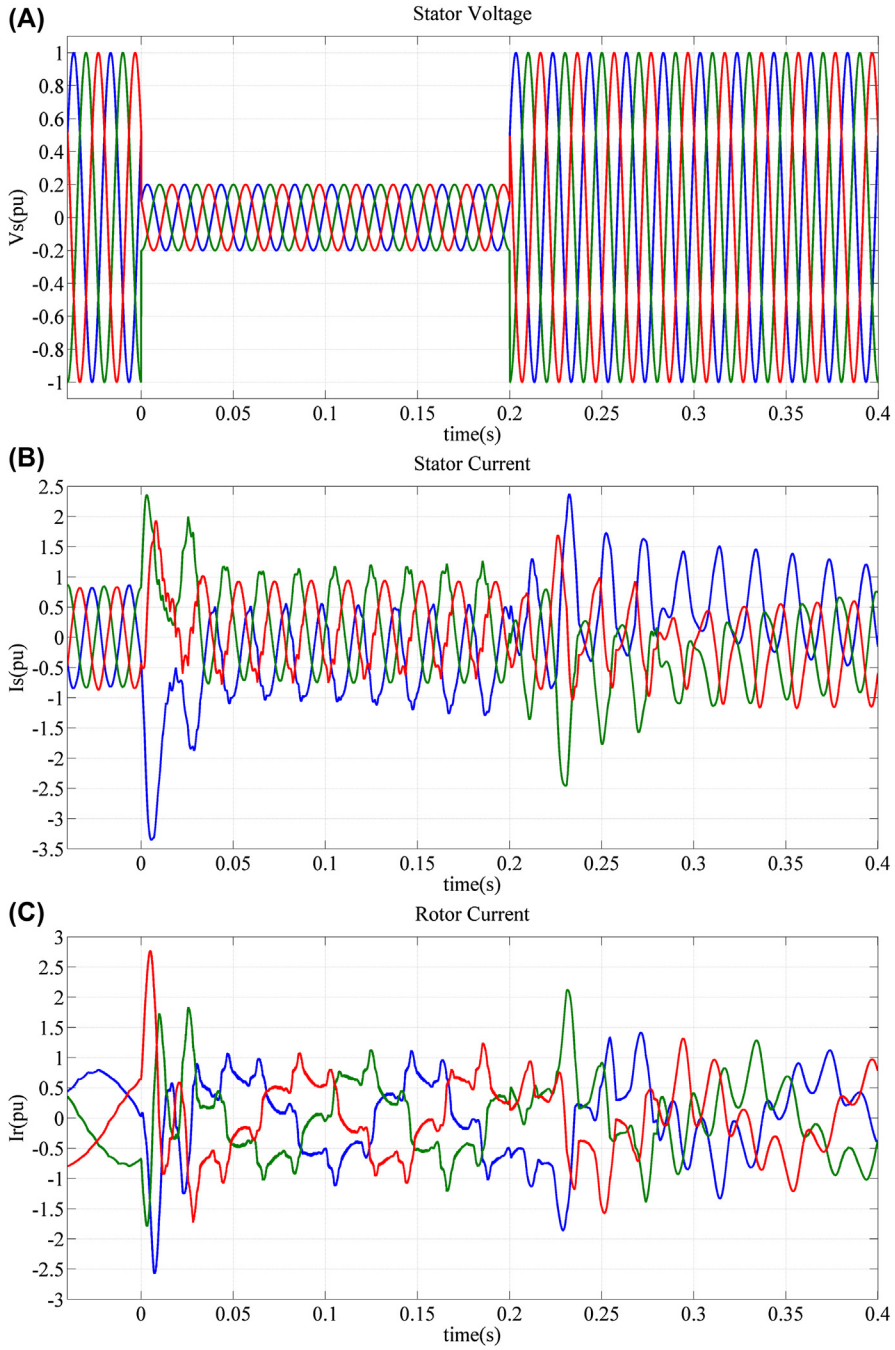

FIGURE 15.21

Effect of voltage dip on a doubly fed induction generator. (A) Stator voltage, (B) stator current, (C) rotor current, (D) GSC current, (E) DC-link voltage, (F) stator active and reactive power.

Source: Author.

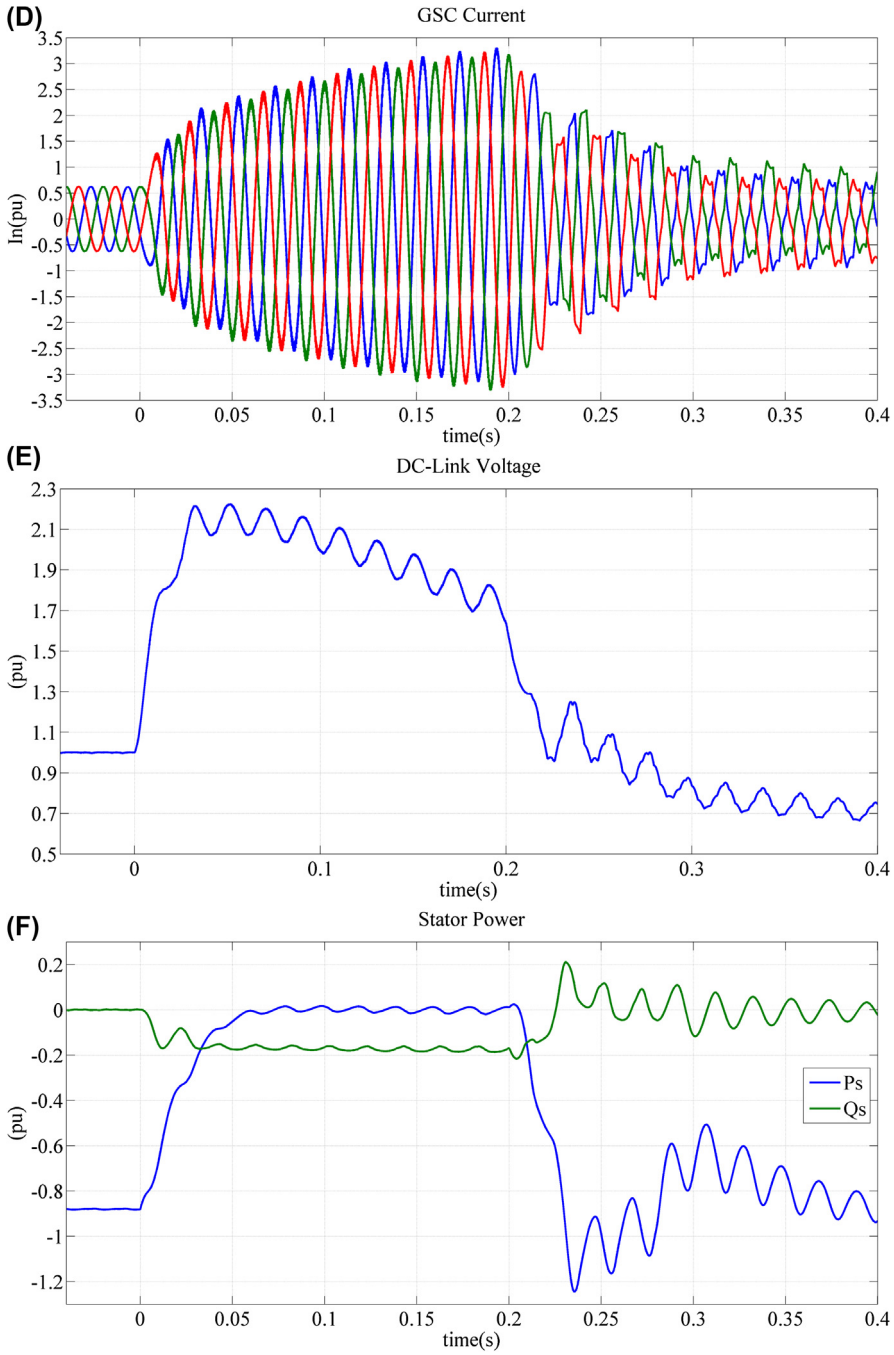

FIGURE 15.21 cont'd.

If there is no change in control operation, GSC will try to stabilize DC-link voltage. To do so, it will force currents far beyond switches' rated values, as shown in the figure. However, even with these attempts, DC-link voltage could not be controlled.

5.2 GRID CODE REQUIREMENTS

In the past, wind turbines were allowed to disconnect from the grid when faults occurred. They were considered as a large industrial load and were subjected to the same standards These requirements aim to protect the machine itself and prevent from islanding operation. Thus, the old codes allowed the disconnection during grid faults, which contributes to the dip.

Nowadays, because of the increasing penetration of these sources in electrical power system, national grid codes understand that they must contribute to the stability during these disturbances, as any other power source. For the proper operation of electrical power system, it is essential that all generators connected to the grid support and help to mitigate oscillations in voltage and frequency. A simultaneous disconnection of a large amount of wind turbines at the same time may collapse system stability in that region.

As stated before, the voltage dips are especially problematic to the WECS. Thus, there are specific requirements in each national grid code concerning wind turbines supportability during these faults, and the codes show the regions that the turbine shall still stay connected with. These regions are determined by the depth of the voltage dip and its duration [16]. IEC 61400−21 [17] states tests to be applied to a wind turbine, as detailed in Table 15.1.

Table 15.1 IEC 61400−21 Voltage Dip Tests

Case	Voltage Magnitude After the Dip (pu)	Positive Sequence Voltage Magnitude (pu)	Duration (s)
VD1—Three-phase symmetric voltage dip	0.90 ± 0.05	0.90 ± 0.05	0.50 ± 0.02
VD2—Three-phase symmetric voltage dip	0.50 ± 0.05	0.50 ± 0.05	0.50 ± 0.02
VD3—Three-phase symmetric voltage dip	0.20 ± 0.05	0.20 ± 0.05	0.20 ± 0.02
VD4—Phase−phase voltage dip	0.90 ± 0.05	0.95 ± 0.05	0.50 ± 0.02
VD5—Phase−phase voltage dip	0.50 ± 0.05	0.75 ± 0.05	0.50 ± 0.02
VD6—Phase−phase voltage dip	0.20 ± 0.05	0.60 ± 0.05	0.20 ± 0.02

Source: Author.

In addition, to help voltage restoration during a fault, some countries demand that WECS provide reactive power for the grid. Inserting reactive power, DFIG will operate with leading power factor and help the voltage to increase. Grid codes have, also, curves to determine the amount of reactive current to be injected, according to the voltage dip depth.

5.3 CROWBAR PROTECTION

In a general way, crowbar is a widely used device in power electronics circuit protection against overvoltages. In DFIG-based WECS, the term describes any device that provides an alternative path to the currents, diverting then from the RSC, through a low-resistance circuit. It is activated when any sign of a fault is detected, such as overcurrent in the rotor, low stator voltage, or overvoltage in the DC-link. The activation of Crowbar protection is temporary; it means during normal operation Crowbar is off, during a fault it is activated, and after the fault clearance it is turned off again.

The use of crowbar in wind turbines is reported even before the grid code requirements for WECS low-voltage ride-through. There are some variations in the implementation of this technology, as discussed before. However, because of its simplicity and as it is a well-known and reliable solution, it remains being the main solution in many wind farms all over the world.

Despite its wide-spread utilization, Crowbar presents some disadvantages. When it is activated, the machine is no longer controlled by the RSC—which means it lost control for this period. Also, the power system seems DFIG as a wound rotor machine with a high rotor resistance and a very high slip. This configuration consumes much reactive power from a grid already disturbed, making it even more difficult for the voltage to be restored. In addition, as crowbar is a resistance, much energy is wasted within its activation.

5.4 COMPLEMENTARY PROTECTION

5.4.1 Pitch Angle Control

One of the issues during a voltage dip is that the power cannot be delivered to the electrical grid. This method uses a control that regulates the angle between the blades and the wind force [18]. This way, the power extraction from the wind is reduced preventing major damages to the WECS. However, this variation in blade angles, especially in large turbines, demands much time compared with electrical transients.

This approach has been applied in almost every WECS as a solution for steady-state condition, together with another technique with faster response, which will act during the transient phase. The pitch angle control, alone, is not able to accomplish grid code requirements and protect DFIG system.

5.4.2 Chopper Circuit

To protect DC-link, the most common protection is the chopper circuit. It consists of a resistance in parallel with DC-bus capacitor, which is switched on when high

voltage is detected [19]. This resistance enables an alternative path to hazardous currents in the capacitor and regulates its voltage. Usually, chopper circuit is placed as a complementary circuit to the crowbar protection.

5.5 ALTERNATIVE SOLUTIONS

Because of the theme relevance, a great number of solutions were and are being proposed. Some of these solutions have already been well established and implemented on wind turbines, many others still need maturation and substantiation. In general, a comprehensive fault ride-through technique should pursue the following main goals:

- Minimize the voltage drop at the generator
- Divert or negate rotor overcurrent
- Produce appropriate power output during faults.

5.5.1 Control Strategies

Many works propose ride-through improvement by using control strategies of the rotor currents produced by the power electronic converter.

Some strategies inject currents by RSC to oppose natural and negative sequence components of magnetic flux [20], or in counterphase with stator currents [21], and thus limit the currents levels on the converter circuit. The great benefit of this kind of solution is that no additional hardware is used, which considerably reduces costs. However, these proposals still have to improve its current limitation and the reactive power consumption during the fault. Also, all these methods have a great dependence on machine parameters to adequate control operation, which in practice reduces reliability, once these parameters vary over time and cannot be ever precisely measured.

5.5.2 Hardware Solutions

Because of the great relevance of the fault supportability issue and the drawbacks of both crowbar solutions and control strategies, alternative hardware solutions have been proposed in literature. The idea behind these proposals is that if an external power electronic device is used to compensate the faulty grid voltage, any protection method in the DFIG system can be left out.

One of the most prominent solution is the Dynamic Voltage Restorer (DVR), which is a voltage source converter connected in series to the grid to correct faulty line voltages. There are several topologies for DVR implementation [22] and many works attest that this proposal is feasible as a protection for WECS, both in squirrel-cage generators [23] as in DFIG systems [24].

Lately, solutions applying superconductive materials have been proposed. These materials have singular characteristics of resistance and inductance change during fault conditions, which are used in DFIG benefit. Some of them implement Superconducting Magnetic Energy Storage to protect the whole wind farm [25] or in individual DFIG [26], others propose resistive Superconductor Fault Current Limiter placed in the point of connection between DFIG and the grid [27] or in the rotor

circuit [28]. However, the superconductor material needs a cryogenic system to operate and none of the proposals experimentally demonstrate its performance.

The disadvantages of any of these hardware solutions are the cost and the reduction of system reliability with the increase in the number of electronic devices, although, much research has been made on new proposals on topologies, technologies, and on their control to enhance DFIG performance during grid faults.

REFERENCES

[1] G.A. Smith, K.A. Nigim, Wind-energy recovery by a static Scherbius induction generator, IEE Proc. C 128 (6) (1981).

[2] R. Pena, J.C. Clare, G.M. Asher, Doubly fed induction generator using back-to-back PWM converters and its application to variable-speed wind-energy generation, IEE Proc.-Electr. Power Appl. 143 (3) (1996) 231−241.

[3] J.G. Slootweg, et al., General model for representing variable speed wind turbines in power system dynamics simulations, IEEE Trans. Power Syst. 18 (1) (2003) 144−151.

[4] R. Teodorescu, M. Liserre, P. Rodriguez, Grid Converters for Photovoltaic and Wind Power Systems, vol. 29, John Wiley & Sons, 2011.

[5] H. Polinder, et al., Trends in wind turbine generator systems, IEEE J. Emerg. Sel. Top. Power Electron. 1 (3) (2013) 174−185.

[6] P.C. Krause, O. Wasynczuk, S. Sudhoff, Analysis of Electric Machinery and Drive Systems, IEEE Press, 2002.

[7] A.E. Fitzgerald, et al., Electric Machinery, vol. 5, McGraw-Hill, New York, 2003.

[8] A. Petersson, Analysis, Modeling and Control of Doubly-Fed Induction Generators for Wind Turbines, Chalmers University of Technology, 2005.

[9] J.M. Carrasco, et al., Power-electronic systems for the grid integration of renewable energy sources: a survey, IEEE Trans. Ind. Electron. 53 (4) (2006) 1002−1016.

[10] M. Liserre, et al., Overview of multi-MW wind turbines and wind parks, IEEE Trans. Ind. Electron. 58 (4) (2011) 1081−1095.

[11] K.E. Okedu, et al., Wind farms fault ride through using DFIG with new protection scheme, IEEE Trans. Sustain. Energy 3 (2) (2012) 242−254.

[12] M. Benbouzid, S. Muyeen, F. Khoucha, An up-to-date review of low-voltage ride-through techniques for doubly-fed induction generator-based wind turbines, Int. J. Energy Convers. 3 (1) (2015) 1−9.

[13] V. Yaramasu, et al., High-power wind energy conversion systems: state-of-the-art and emerging technologies, Proc. IEEE 103 (5) (2015) 740−788.

[14] F. Blaabjerg, K. Ma, Future on power electronics for wind turbine systems, IEEE J. Emerg. Sel. Top. Power Electron. 1 (3) (2013) 139−152.

[15] I. Erlich, H. Wrede, C. Feltes, Dynamic behavior of DFIG-based wind turbines during grid faults, in: Power Conversion Conference-Nagoya, 2007. PCC'07, IEEE, 2007.

[16] M. Tsili, S. Papathanassiou, A review of grid code technical requirements for wind farms, IET Renew. Power Gener. 3 (3) (2009) 308−332.

[17] Standard, IEC 61400−61421, Measurement and Assessment of Power Quality of Grid Connected Wind Turbines, 2001.

[18] T. Senjyu, et al., Output power leveling of wind turbine generator for all operating regions by pitch angle control, IEEE Trans. Energy Convers. 21 (2) (2006) 467−475.

[19] G. Pannell, et al., Evaluation of the performance of a DC-link brake chopper as a DFIG low-voltage fault-ride-through device, IEEE Trans. Energy Convers. 28 (3) (2013) 535−542.
[20] S. Xiao, et al., An LVRT control strategy based on flux linkage tracking for DFIG-based WECS, IEEE Trans. Ind. Electron. 60 (7) (2013) 2820−2832.
[21] F.K.A. Lima, et al., Rotor voltage dynamics in the doubly fed induction generator during grid faults, IEEE Trans. Power Electron. 25 (1) (2010) 118−130.
[22] J.G. Nielsen, F. Blaabjerg, A detailed comparison of system topologies for dynamic voltage restorers, IEEE Trans. Ind. Appl. 41 (5) (2005) 1272−1280.
[23] D. Ramirez, et al., Low-voltage ride-through capability for wind generators based on dynamic voltage restorers, IEEE Trans. Energy Convers. 26 (1) (2011) 195−203.
[24] C. Wessels, F. Gebhardt, F.W. Fuchs, Fault ride-through of a DFIG wind turbine using a dynamic voltage restorer during symmetrical and asymmetrical grid faults, IEEE Trans. Power Electron. 26 (3) (2011) 807−815.
[25] A.M. Shiddiq Yunus, M.A.S. Masoum, A. Abu-Siada, Application of SMES to enhance the dynamic performance of DFIG during voltage sag and swell, IEEE Trans. Appl. Supercond. 22 (4) (2012) 5702009.
[26] W. Guo, L. Xiao, S. Dai, Enhancing low-voltage ride-through capability and smoothing output power of DFIG with a superconducting fault-current limiter−magnetic energy storage system, IEEE Trans. Energy Convers. 27 (2) (2012) 277−295.
[27] M.E. Elshiekh, D.-E.A. Mansour, A.M. Azmy, Improving fault ride-through capability of DFIG-based wind turbine using superconducting fault current limiter, IEEE Trans. Appl. Supercond. 23 (3) (2013) 5601204.
[28] F. Oliveira, et al., Enhancing LVRT of DFIG by using a superconducting current limiter on rotor circuit, Energies. 9 (1) (2015) 16.